# Multi-Vector Fluorescence Analysis of the *xpt* Guanine Riboswitch Aptamer Domain and the Conformational Role of Guanine[†]

Michael D. Brenner,[‡] Mary S. Scanlan,[‡] Michelle K. Nahas,[§]

Taekjip Ha,[‡,§,¶,*] and Scott K. Silverman[‡,*]

[‡]*Department of Chemistry,* [§]*Department of Physics and Center for the Physics of Living Cells, University of Illinois at Urbana–Champaign, Urbana, Illinois 61801*

*and* [¶]*Howard Hughes Medical Institute, Urbana, Illinois 61801*

**Figure S1.** In-line probing assays for the three aptamer domain variants. (A) P1-P2 variant. (B) P1-P3 variant. (C) P2-P3 variant. See Experimental Procedures for assay (*37*) and quantitation methods. The numbered single-stranded regions show the expected decreases in cleavage in the presence versus absence of 1 μM guanine (G versus –; gold vs. black line graphs to the right of each gel image). In contrast, 1 μM adenine has no effect. Control regions marked "C" show little dependence upon guanine. In the line graphs, the peak marked "n" was used for normalization of the – and G data. Collectively, the in-line probing data confirm that Cy3/Cy5 dye labeling of the variants does not significantly impact their ability to bind guanine. Precise $K_d$ values for guanine for the labeled variants were not determined; we cannot rule out modest changes in $K_d$ due to the presence of the dyes. In particular, P2-P3 shows less guanine-dependent protection than do the other two variants. Nevertheless, P2-P3 does show a substantial FRET change upon introduction of guanine (Figure 4), indicating that significant guanine binding still occurs. P1-P2 and P1-P3 were each probed using an RNA that has an unhybridized 5′-overhang, corresponding directly to the RNA used in the ensemble FRET measurements. For P2-P3, the illustrated data were obtained with an RNA that altogether lacks the 5′-overhang; essentially equivalent data were obtained using the RNA that has an unhybridized 5′-overhang (data not shown). In the illustrated data, region 4 of P2-P3—in particular, the lowest band that, by comparison with the P1-P2 and P1-P3 data, is expected to decrease most in intensity upon guanine binding—could not be fully resolved and quantified due to its proximity to the 5′-terminus.

**Figure S2.** Purine specificity for the conformational changes observed in the P1-P2 variant. Data are similar to the histograms of Figure 2C, except that 500 nM or 50 μM adenine was included as indicated (all in the absence of $Mg^{2+}$).

**Figure S3.** Comparison of smFRET data for the P1-P2 and P2-P3 variants. (A) Rate comparison of P1-P2 and P2-P3 at 10 μM $Mg^{2+}$. The high ($E$ >0.5) and low ($E$ <0.5) FRET dwell times for the P1-P2 variant were recorded without (left) and with (right) 500 nM guanine at 10 μM $Mg^{2+}$. The inverse dwell times for high and low FRET values ($k_{unfold}$ and $k_{fold}$) were plotted for both P1-P2 and P2-P3. Without and with guanine, respectively, 171 and 101 P1-P2 variant molecules were analyzed to obtain $k_{unfold}$ and $k_{fold}$. (B) Heterogeneity in dynamics of P1-P2 and P2-P3. The average transition rates shown in panel A indicate a contribution from fast (>1 $s^{-1}$) FRET fluctuations for the P1-P2 variant. On the left are depicted representative traces in the absence of $Mg^{2+}$ and guanine exhibiting fast dynamics for P1-P2 and both fast and slow (<1 $s^{-1}$) dynamics for P2-P3. On the right, the distributions of fast, slow, and mixed dynamics are presented for P1-P2 and P2-P3 with different concentrations of $Mg^{2+}$ and guanine. In all conditions analyzed, over 50% of P1-P2 traces exhibited only slow dynamics, while a majority of the traces for the P2-P3 variant displayed both fast and slow dynamics. Both variants are capable of fast dynamics, but P2-P3 exhibits more heterogeneity within individual traces. Therefore, the average trace for the P1-P2 variant differs from the average trace for P2-P3 variant in terms of dynamic behavior, although the average FRET dwell times and the transition rates for both variants are comparable.

**Figure S4.** Stabilization by guanine of the high-$E$ state of the P2-P3 variant. At each $Mg^{2+}$ and guanine concentration, the value of ΔG° was calculated as $-RT \cdot \ln(k_{fold}/k_{unfold})$. Guanine stabilizes the high-FRET state by $\Delta\Delta G° = 0.51 \pm 0.26$ kcal/mol at 100 μM $Mg^{2+}$ and $0.44 \pm 0.40$ kcal/mol at 1 mM $Mg^{2+}$. Error bars represent propagation of the standard errors of $k$ values from Figure 4E.

**Figure S5.** Heterogeneity in the folded-state and unfolded-state dwell times of the G riboswitch aptamer domain. (A) The high-*E* (folded state) and low-*E* (unfolded state) dwell times were averaged to yield a single value for each of the indicated number of P2-P3 molecules under each buffer condition. The results are represented in 2D scatter plots that compare the average time each molecule spent in the folded or unfolded state during data acquisition (~1 min) (*17*). (B) Scatter plots were constructed for the P1-P2 variant with and without 500 nM guanine at 10 μM $Mg^{2+}$. The log averages of the folded-state and unfolded-state dwell time values for all molecules under each condition were calculated to determine the average high-FRET and low-FRET dwell times as well as the values for $k_{fold}$ and $k_{unfold}$ (Figures 4E and S3A).

Figure S1. In-line probing assays for the three aptamer domain variants.

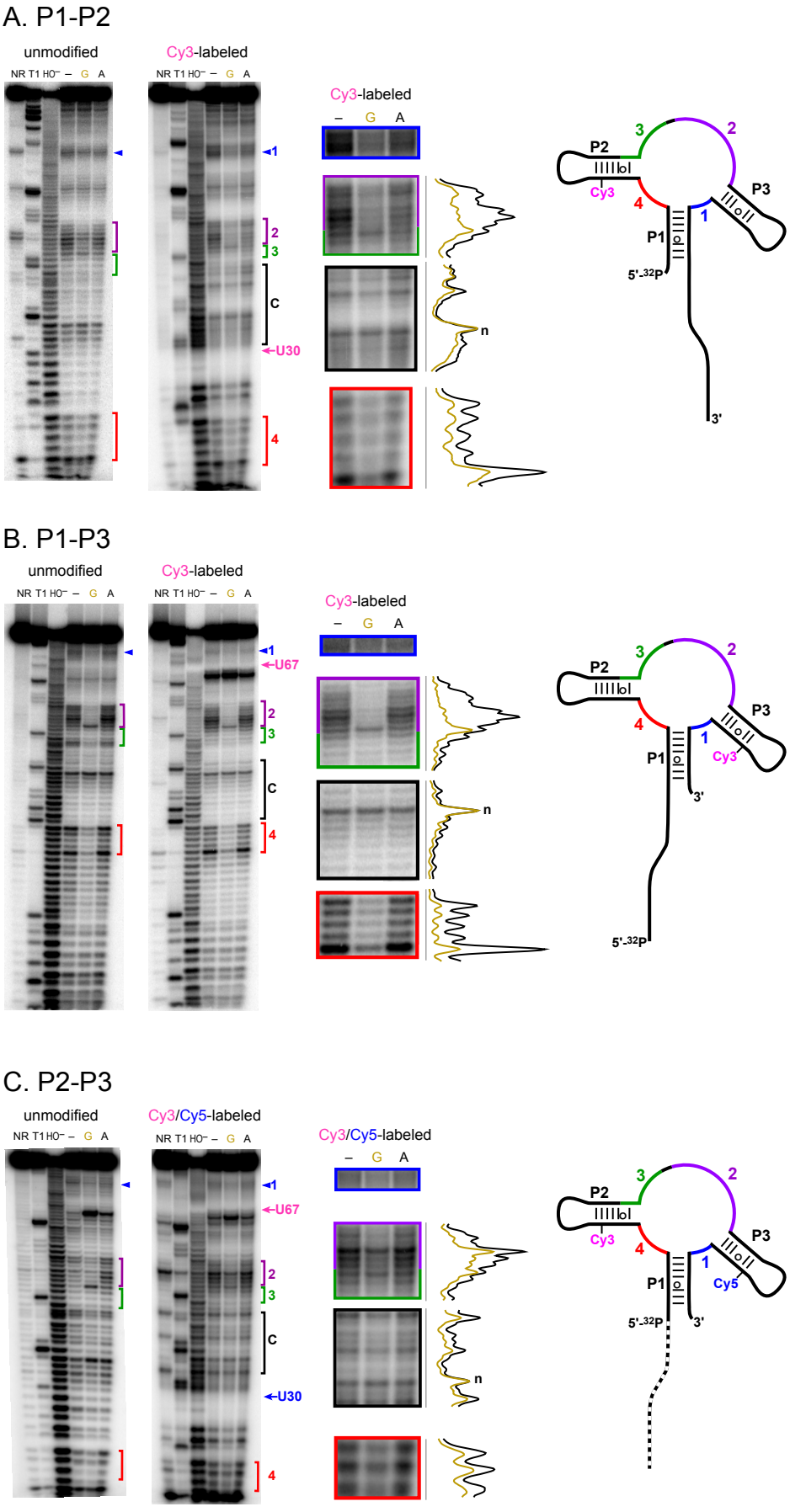

Figure S2. Purine specificity for the conformational changes observed in the P1-P2 variant.

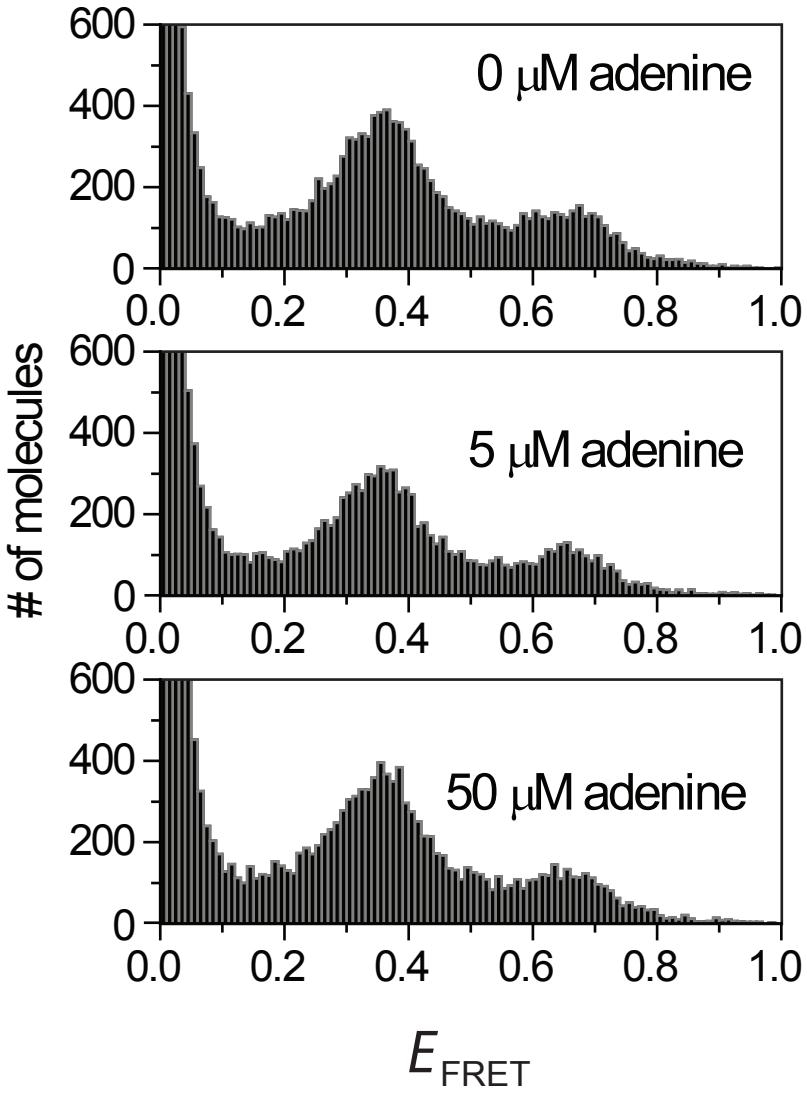

Figure S3. (A) Rate comparison of P1-P2 and P2-P3 at 10 μM $Mg^{2+}$.

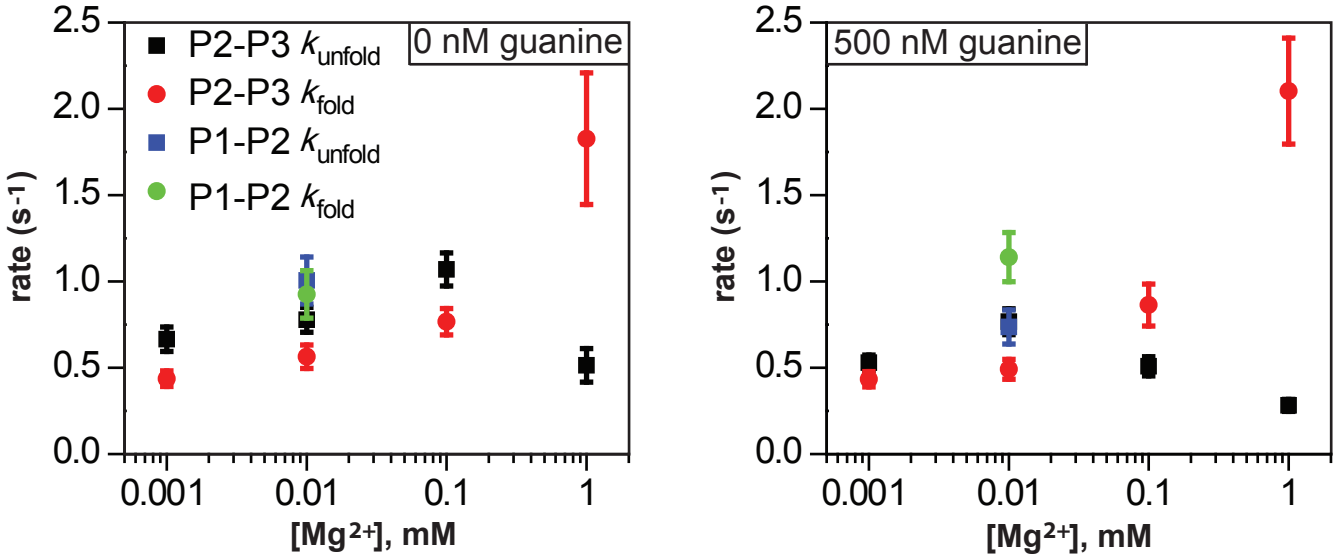


(B) Heterogeneity in dynamics of P1-P2 and P2-P3.

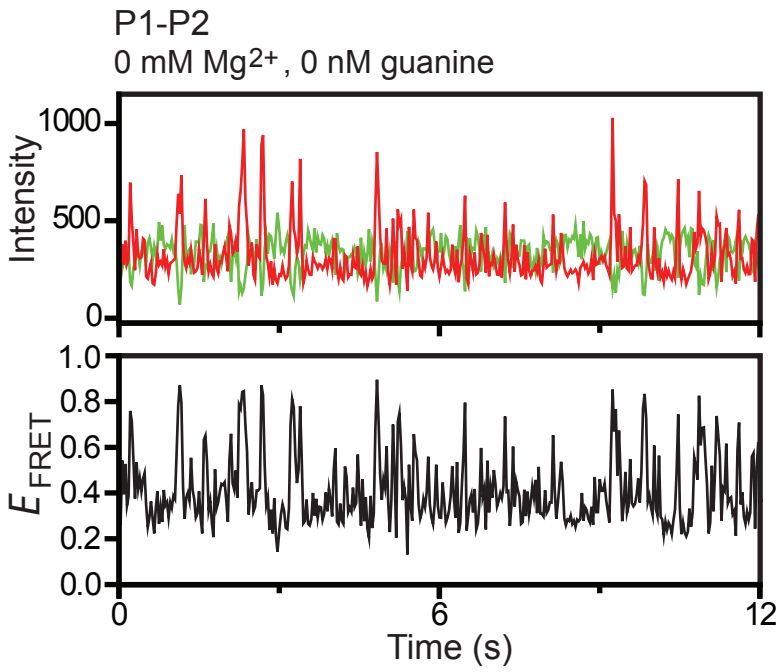


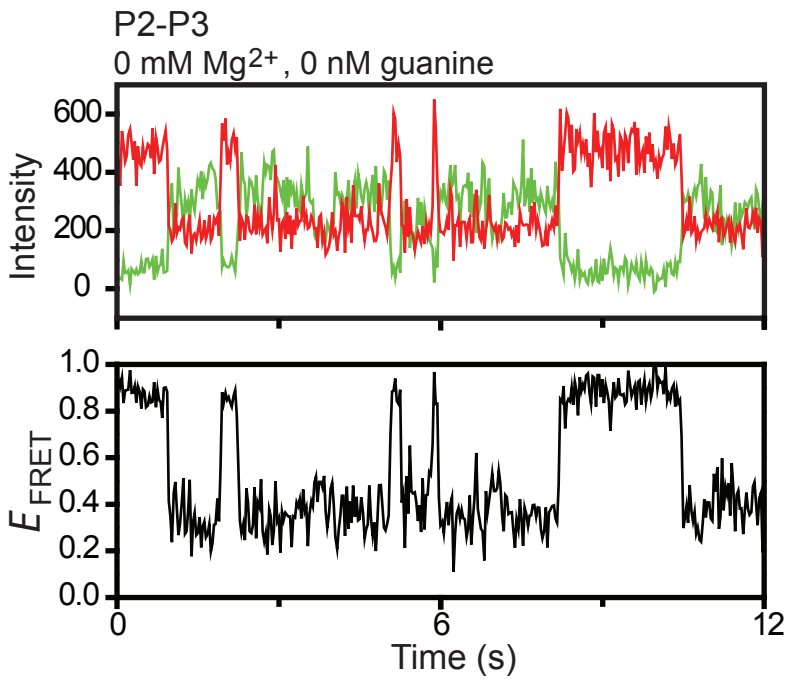


Survey of P1-P2 dynamic behavior

| Buffer | % slow | % fast | % both |
|---|---|---|---|
| 0 μM $Mg^{2+}$ 0 nM G | 53.4 | 29.5 | 17.0 |
| 10 μM $Mg^{2+}$ 0 nM G | 62.1 | 17.4 | 20.5 |
| 0 μM $Mg^{2+}$ 500 nM G | 60.0 | 13.3 | 26.7 |
| 10 μM $Mg^{2+}$ 500 nM G | 53.2 | 24.2 | 22.6 |

Survey of P2-P3 dynamic behavior

| Buffer | % slow | % fast | % both |
|---|---|---|---|
| 0 μM $Mg^{2+}$ 0 nM G | 19.6 | 15.9 | 64.5 |
| 0 μM $Mg^{2+}$ 500 nM G | 19.3 | 16.9 | 63.9 |

Figure S4. Stabilization by guanine of the high-*E* state of the P2-P3 variant.

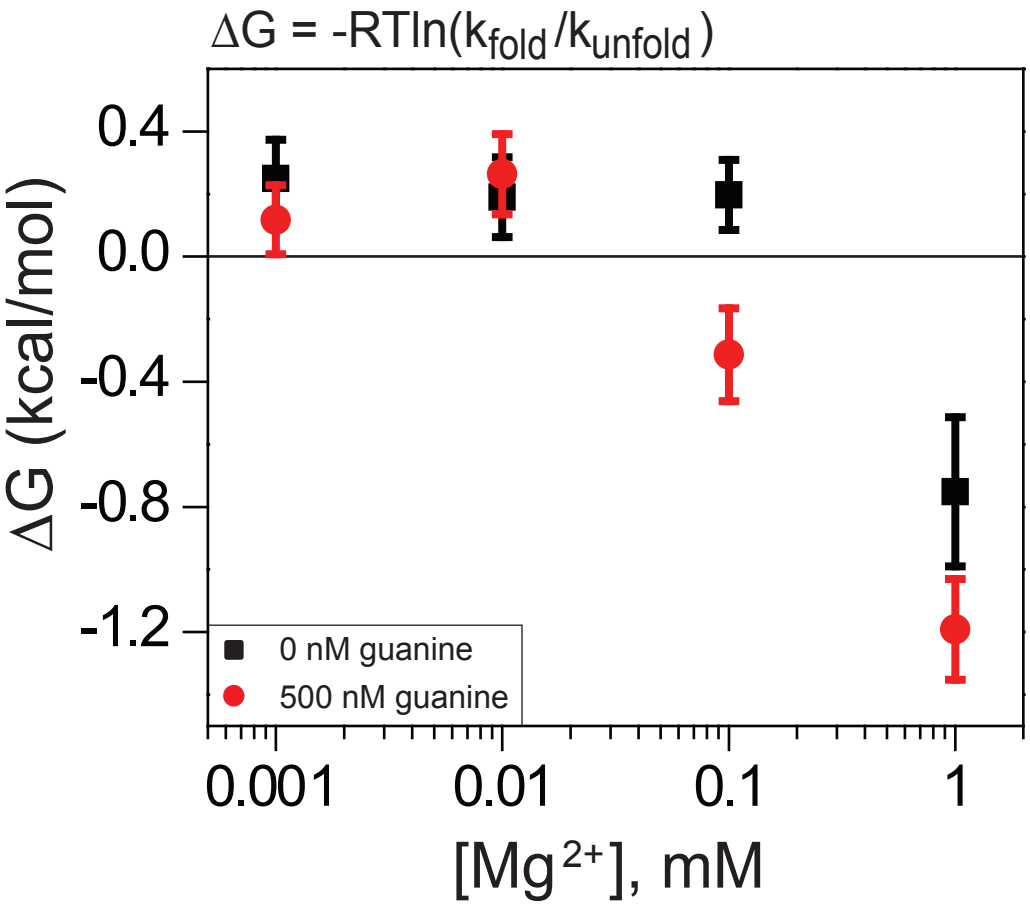

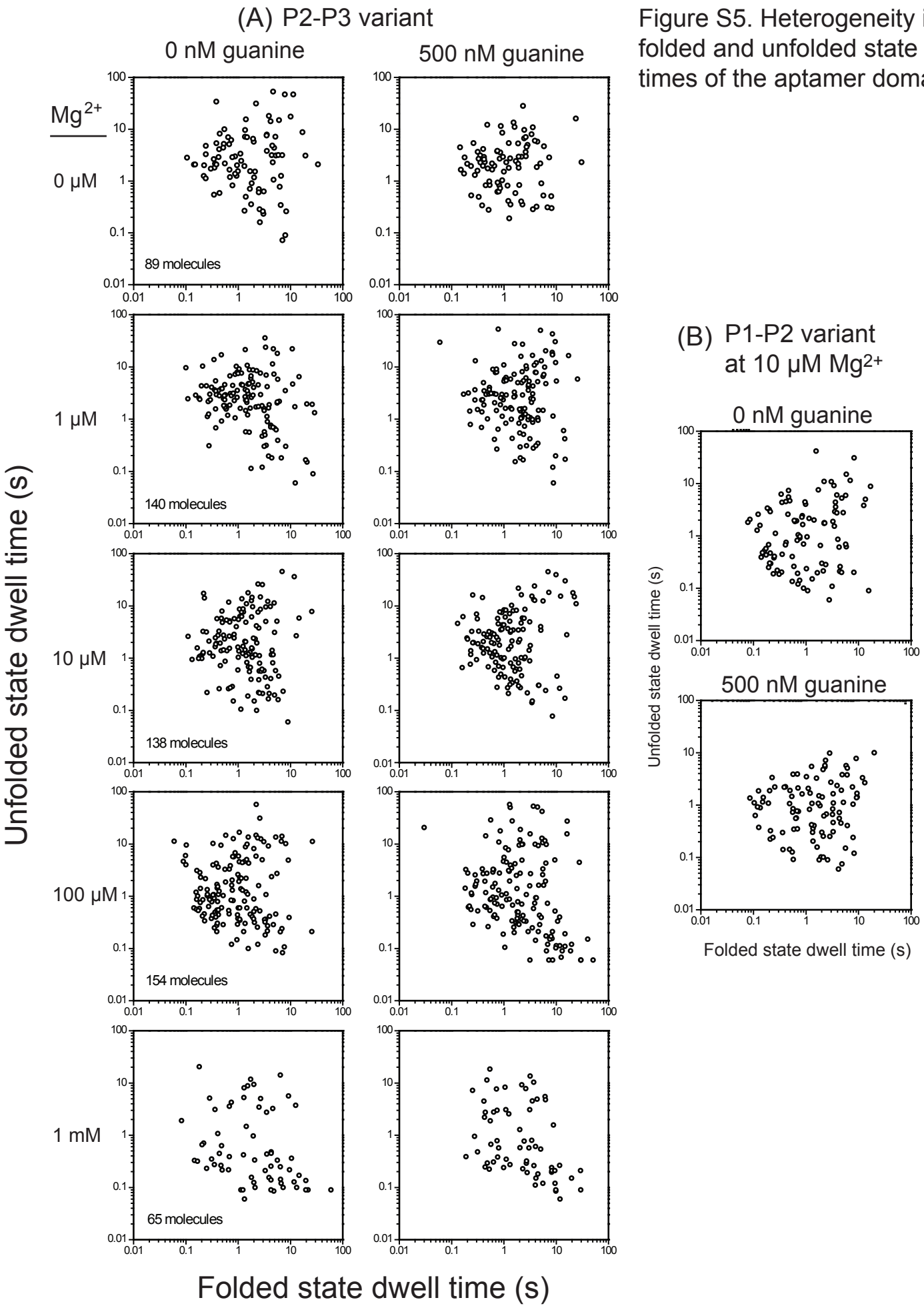


Figure S5. Heterogeneity in the folded and unfolded state dwell times of the aptamer domain.